Antioxidation and DNA-Binding Properties of Binuclear Lanthanide(III) Complexes with a *Schiff* Base Ligand Derived from 8-Hydroxyquinoline-7-carboxaldehyde and Benzoylhydrazine

by **Yongchun Liu***, **Kejun Zhang**, **Yun Wu**, **Junying Zhao**, and **Jianning Liu**

College of Chemistry and Chemical Engineering, Key Laboratory of Longdong Biological Resources in Gansu Province, Longdong University, Qingyang, Gansu 745000, P. R. China
(phone: 86-934-6466862; e-mail: ychliu001@163.com)

8-Hydroxyquinoline-7-carboxaldehyde (8-HQ-7-CA), *Schiff*-base ligand 8-hydroxyquinoline-7-carboxaldehyde benzoylhydrazone, and binuclear complexes $[LnL(NO_3)(H_2O)_2]_2$ were prepared from the ligand and equivalent molar amounts of $Ln(NO_3)\cdot 6\,H_2O$ ($Ln = La^{3+}$, Nd^{3+}, Sm^{3+}, Eu^{3+}, Gd^{3+}, Dy^{3+}, Ho^{3+}, Er^{3+}, Yb^{3+}, resp.). Ligand acts as dibasic tetradentates, binding to Ln^{III} through the phenolate O-atom, N-atom of quinolinato unit, and C=N and –O–C=N– groups of the benzoylhydrazine side chain. Dimerization of this monomeric unit occurs through the phenolate O-atoms leading to a central four-membered $(LnO)_2$ ring. Ligand and all of the Ln^{III} complexes can strongly bind to CT-DNA through intercalation with the binding constants at 10^5–10^6 M^{-1}. Moreover, ligand and all of the Ln^{III} complexes have strong abilities of scavenging effects for hydroxyl ($HO^{\bullet}$) radicals. Both the antioxidation and DNA-binding properties of Ln^{III} complexes are much better than that of ligand.

Introduction. – DNA is one of the primary intracellular targets of anticancer drugs due to the interaction of small molecules with it, causing DNA damage in cancer cells, inhibiting the division of cancer cells, and resulting in cell death [1]. Some DNA binders are effective inhibitors of the formation of a DNA/TBP complex or topoisomerases. Adding a reactive entity endowed with oxidative properties should improve the efficiency of inhibitors [2].

Previously, we investigated the biological properties of lanthanide(III) complexes with *Schiff* base ligands derived from 8-hydroxyquinoline-2-carboxaldehyde and some aroylhydrazines. It was found that all these ligands and rare earth metal complexes showed strong antioxidation and DNA-binding properties, and they might be used as potential anticancer drugs [3]. In this study, the *Schiff* base ligand derived from 8-hydroxyquinoline-7-carboxaldehyde with benzoylhydrazine and its Ln^{III} complexes were prepare to investigate their antioxidation and DNA-binding properties.

Results and Discussion. – 8-Hydroxyquinoline-7-carboxaldehyde (8-HQ-7-CA) was prepared according literature procedures with small modifications [4]. The *Schiff* base ligand 8-hydroxyquinoline-7-carboxaldehyde benzoylhydrazone (H_2L; **1**) was prepared from equivalent molar amounts of 8-HQ-7-CA and benzoylhydrazine (*Scheme*). Then, its nine Ln^{III} complexes **2**–**10** were prepared from the ligand and equivalent molar amounts of $Ln(NO_3)\cdot 6\,H_2O$ ($Ln = La^{3+}$, Nd^{3+}, Sm^{3+}, Eu^{3+}, Gd^{3+}, Dy^{3+}, Ho^{3+}, Er^{3+}, Yb^{3+}, resp.). All the Ln^{III} complexes are yellow powders, stable in

air, and soluble in DMF and DMSO, but slightly soluble in MeOH, EtOH, MeCN, AcOEt and acetone, THF and $CHCl_3$. They are 1:1 metal-to-ligand (stoichiometry) complexes and act as non-electrolytes [5].

Scheme 1. *The Synthetic Route to Ligand* **1**

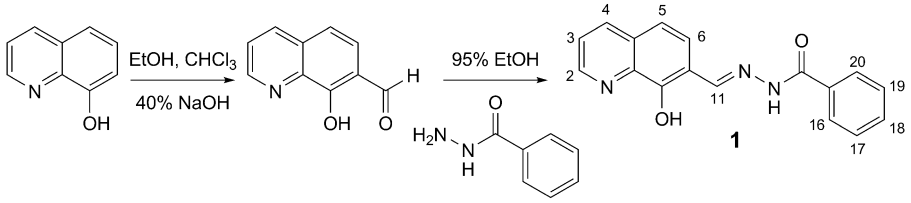

The characteristic IR bands (cm^{-1}) at 3328, 3206, 1641, 1597, 1571, and 1288 of ligand can be assigned to $\tilde{\nu}$(NH), $\tilde{\nu}$(OH), $\tilde{\nu}$(CO), $\tilde{\nu}$(C=N, azomethine), $\tilde{\nu}$(C=N, pyridine), and ν(C–OH), respectively. Careful comparison with the characteristic IR bands of the ligand and Ln^{III} complexes led to the following conclusions: *1*) Bands at 3412–3387 (br.) assigned to $\tilde{\nu}$(OH) of H_2O, at 965–960_w assigned to $\rho_r(H_2O)$, and at 642–633_w assigned to ρ_w (H_2O) indicate that coordinated H_2O molecules participate in the Ln^{III} complexes. *2*) Bands at 1099–1094 assigned to $\tilde{\nu}$(C–OM) indicate that the binding of every metal ion to ligand through an O–M linkage takes place [6]. *3*) Bands at 1641*s* assigned to $\tilde{\nu}$(CO) and at 3328v*s* assigned to $\tilde{\nu}$(NH) of benzoylhydrazine side chain of ligand have disappeared in the IR spectra of Ln^{III} complexes, indicating that they participate in the Ln^{III} complexes with the O=C–NH– group, possibly undergoing enolization and deprotonation to –O–C=N–. *4*) Bands at 1603–1590 assigned to $\tilde{\nu}$(CN) of azomethines of the Ln^{III} complexes were shifted by 6–4 cm^{-1}, and bands at 1564–1558 assigned to $\tilde{\nu}$(CN) of pyridines of the Ln^{III} complexes were shifted by 7–13 cm^{-1} in comparison with those of the ligand, indicating that both N-atoms of azomethines and pyridines participate in the complexes. *5*) Bands at 537–531*w* assigned to $\tilde{\nu}$(MO) and at 447–428*w* assigned to $\tilde{\nu}$(MN) of the Ln^{III} complexes further indicate that the O- and N-atoms participate in complexes. *6*) All the Ln^{III} complexes exhibit bands at 1469–1465 (ν_1), 1326–1317 (ν_4), 1036–1031 (ν_2), 838–836 (ν_3), 726–716 (ν_5), and $\Delta\nu(\nu_1-\nu_4)$ 149–144 cm^{-1}, indicating that nitrate ions bidentately participate in the Ln^{III} complexes [7].

The results of elemental analyses, molar conductance, IR spectra, and ESI-MS data indicate that ligand acts as a dibasic tetradentate, binding to Ln^{III} through the phenolate O-atom, N-atom of quinolinato unit, and C=N group and –O–C=N– groups (enolized and deprotonated from O=C–NH–) of the benzoylhydrazine side chain. Dimerization of this monomeric unit may occur through the phenolate O-atoms leading to a central four-membered $(LnO)_2$ ring. All the metal complexes are structurally similar to each other, and the suggested binuclear composition is $[LnL(NO_3)(H_2O)_2]_2$ (*Fig. 1*). However, the *m*/*z* data (M^+; DMF solution) of complexes indicate that the coordinated H_2O molecules of powder Ln^{III} complex can be replaced by DMF molecules, when it is dissolved in DMF solution, and that the composition of binuclear complex in DMF solution is of $[LnL(NO_3)(DMF)_2]_2$. Additionally, the *m*/*z* data ([*M*/

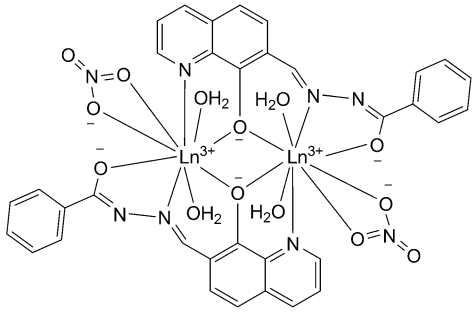

Fig. 1. *The suggested binuclear structures of Ln^{III} complexes*

2]$^+$; DMF solution) of complex can also be found, indicating that there exists a monomeric unit in DMF solution.

Hydrodynamic measurements that are sensitive to length change of DNA (*i.e.*, viscosity and sedimentation) are regarded as the least ambiguous and the most critical criteria for binding modes in solution in absence of crystallographic structural data [8]. Viscosity measurements are very sensitive to changes in the length of DNA, as viscosity is proportional to L^3 for rod-like DNA of length L. Intercalation involves the insertion of a planar molecule between DNA base pairs, resulting in a decrease in the DNA helical twist and lengthening of the DNA; therefore, intercalators cause the unwinding and lengthening of DNA helix, as base pairs become separated to accommodate the binding compound [9]. Whereas agents bound to DNA through groove binding do not alter the relative viscosity of DNA, agents bound to DNA through electrostatic binding will bend or kink the DNA helix, reducing its effective length and its viscosity, concomitantly [10]. With the increasing ratios of the investigated compounds to DNA (base pairs, bps), the relative viscosities of DNA increase steadily (*Fig. 2*), indicating that intercalation takes place between the investigated compounds and DNA helix. In addition, the increases of relative viscosities of DNA for complexes are more than that for ligand, indicating the extent of the unwinding and lengthening of DNA helix by compounds, and the affinities of compounds binding to DNA.

The UV/VIS spectra of the ligand have two types of absorption bands of λ_{max} at 246 ($\varepsilon = 2.58 \times 10^4$ M^{-1} cm^{-1}) and 348 nm ($\varepsilon = 2.11 \times 10^4$ M^{-1} cm^{-1}), which can be assigned to π–π^* transition of aromatic rings and π–π^* of conjugated aromatic rings, respectively. The UV/VIS spectra of Ln^{III} complexes exhibit two typical bands of λ_{max} in the range of 247–263 ($\varepsilon = 1.93$–3.68×10^4 M^{-1} cm^{-1}) and 343–350 nm ($\varepsilon = 1.44$–32.76×10^4 M^{-1} cm^{-1}), which can be assigned to π–π^* transition of aromatic rings and π–π^* of conjugated aromatic rings, respectively. However, compared with ligand, the new bands of λ_{max} at 401–406 nm for complexes can be assigned to the charge transfer from ligand to metal ions ($L \rightarrow Ln^{3+}$) [3]. Additionally, isosbestic point at 385 nm for ligand and isosbestic points at 460–468 nm for Ln^{III} complexes are observed, indicating that the equilibrium of reaction takes place between compound and DNA. Upon successive addition of CT-DNA (bps), the UV/VIS absorption band of ligand shows a progressive hypochromism of 24.1% at 246 nm and another progressive hypochromism of 31.4% at 348 nm at approximately saturated titration end point with C_{DNA}/C_{ligand}

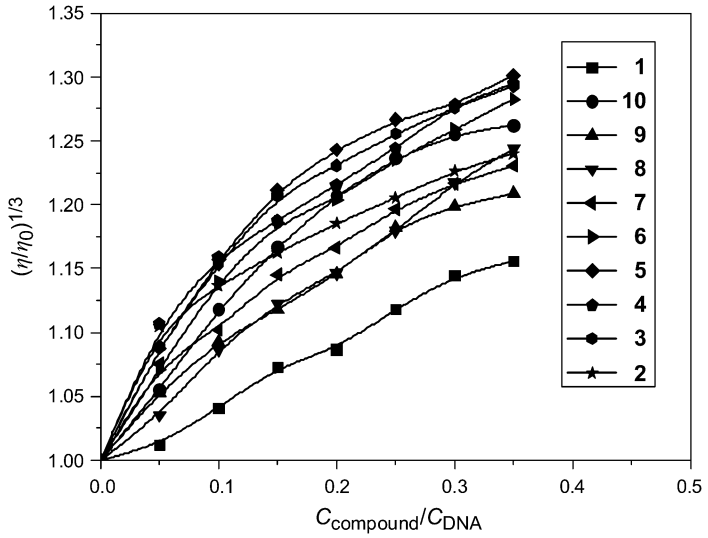

Fig. 2. *Effects of increasing amounts of the investigated compounds on the relative viscosity of CT-DNA*. The concentration of CT-DNA was 50 μM (bps).

1.4 : 1. Similarly, the UV/VIS bands of complexes show a progressive hypochromism of 15.2–72.2% at 247–263 nm and another progressive hypochromism of 12.5–62.5% at 343–350 nm with $C_{DNA}/C_{complex}$ 1.0–1.6 : 1. The obvious hypochromism further indicate the non-covalently intercalative binding of compounds to DNA helix, due to the strong stacking interaction between the aromatic chromophores of the compound and base pairs of DNA [11]. The magnitude of hypochromism is parallel to the intercalative strength and the affinity of a compound binding to DNA [8]. From the UV/VIS titration data, the binding constant (K_b) was determined [12], and the values of K_b are compiled in the *Table*. *Figs. 3–5* show the plots of the UV/VIS titration, the plot of [DNA]/($\varepsilon_f-\varepsilon_a$) *vs.* [DNA] for Dy^{III} complex **7**, and the plot of K_b *vs.* 4f electron number of metal ions, respectively. It is found that Eu^{III} complex **5** presents the strongest binding ability to DNA ($K_b = 26.13 \times 10^5$ M^{-1}) among the investigated compounds (K_b in the range of $26.13–2.938 \times 10^5$ M^{-1}), and that from Gd^{III} to Er^{III} complexes, **6**–**9**, respectively, the values of K_b decrease gradually, while Yb^{III} complex **10** presents higher binding ability, which may be related to the 4f electron effect and the size of metal ions. Additionally, K_b values of DNA binding to ligand and EB (ethidium bromide, classical intercalative agent) are 1.397×10^5 and 0.3068×10^5 M^{-1}, respectively, indicating that all of the Ln^{III} complexes present higher binding abilities to DNA than that of either ligand or EB.

The fluorescence emission intensity of DNA–EB system decreased dramatically upon increasing the amounts of both ligand and Ln^{III} complexes. *Stern–Volmer* equation was used to determine the fluorescent quenching mechanism [9]. Plots of F_o/F *vs.* [Q] are shown in *Fig. 6*, and the quenching data collected and calculated from the good linear relationship when $P < 0.05$ are compiled in the *Table*. The K_{SV} values are in the range of $0.8908–2.694 \times 10^5$ M^{-1} for ligand and Ln^{III} complexes; accordingly, the

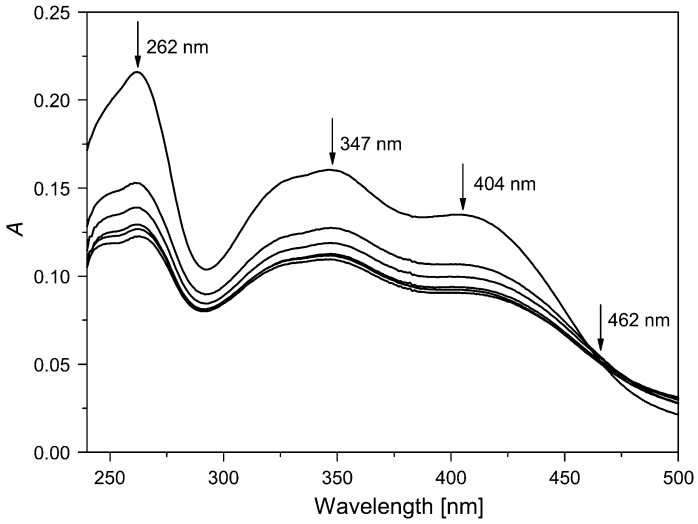

Fig. 3. *Plot of the UV/VIS titration for Dy^{III} complex* (**7**) *by DNA*. Both of the molar concentration of Dy^{III} complex and DNA (bps) are 10.0 μM at approximately saturated titration end point.

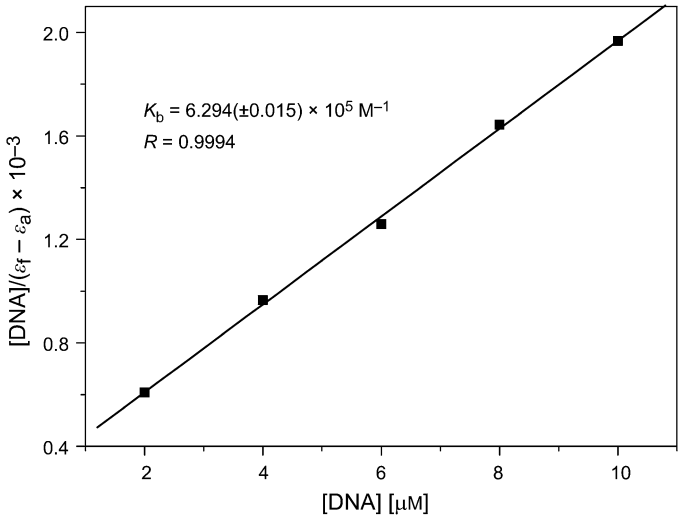

Fig. 4. *Plot of $[DNA]/(\varepsilon_f - \varepsilon_a)$ vs. [DNA] for Dy^{III} complex* (**7**)

corresponding calculated data of K_q are in the range of $4.949-14.97\times10^{12}$ M^{-1} s^{-1}, where the value of τ_o is taken as 1.8×10^{-9} s. All of the current K_q values for the investigated compounds are much greater than $K_{q(max)}$ (2.0×10^{10} M^{-1} s^{-1}), the maximum quenching rate constant of bimolecular diffusion collision, which is indicative of a static type of quenching mechanism arising from the formation of dark complex between the fluorophore and quenching agent [13]. The loss of fluorescence

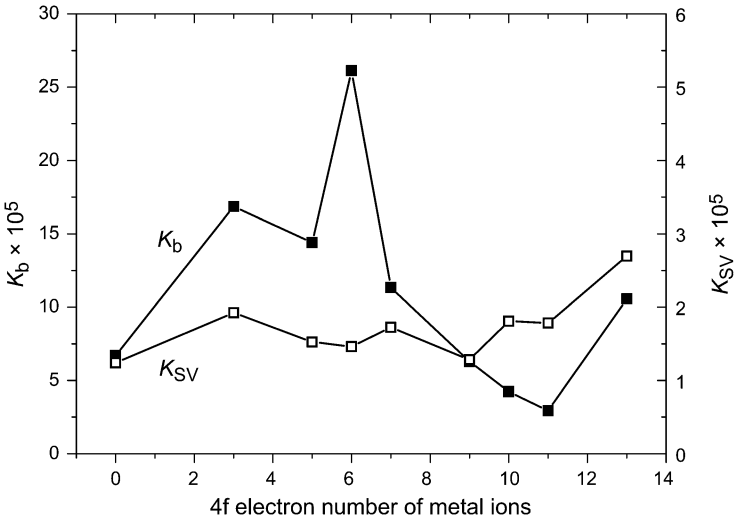

Fig. 5. *Plots of* K_b *and* K_{SV} *vs. 4f electron number of metal ions*

Table 1. *Parameters* K_b, K_{SV}, K_q, FC_{50}, *and* SC_{50} ($OH^{\cdot}$) *for Ligand and* Ln^{III} *Complexes*

	$K_b \times 10^5$ [M^{-1}]	$K_{SV} \times 10^5$ [M^{-1}]	$K_q \times 10^{12}$ [$M^{-1}\ s^{-1}$]	FC_{50} [μM] ($C_{compound}/C_{DNA,nucleotides}$)	SC_{50} [μM] for $HO^{\cdot}$
Ligand **1**	1.397 ± 0.011	0.8908 ± 0.0145	4.949	12.35 (3.088)	21.33 ± 2.51
2	6.708 ± 0.015	1.240 ± 0.025	6.889	8.791 (2.198)	5.675 ± 0.307
3	16.86 ± 0.15	1.925 ± 0.105	10.69	6.393 (1.598)	5.415 ± 0.147
4	14.40 ± 0.15	1.524 ± 0.052	8.467	7.358 (1.839)	5.824 ± 0.194
5	26.13 ± 0.13	1.462 ± 0.036	8.122	7.323 (1.831)	5.515 ± 0.095
6	11.33 ± 0.15	1.724 ± 0.056	9.578	6.913 (1.728)	6.149 ± 0.212
7	6.294 ± 0.015	1.282 ± 0.020	7.122	8.030 (2.008)	7.568 ± 0.347
8	4.236 ± 0.010	1.808 ± 0.041	10.04	6.436 (1.609)	2.499 ± 0.222
9	2.938 ± 0.010	1.783 ± 0.068	9.906	6.571 (1.643)	4.206 ± 0.026
10	10.56 ± 0.13	2.694 ± 0.293	14.97	5.724 (1.431)	4.841 ± 0.030

intensity at the maximum wavelength indicates that most of the EB molecules have been displaced from DNA–EB complex by every quencher at the approximately saturated end point, and that the intercalative binding modes take place between the investigated compounds with DNA [10]. Furthermore, the *Stern–Volmer* dynamic quenching constants, K_{SV}, can also be interpreted as binding affinities of the complexation reaction [14]. The K_{SV} data present the order that is slightly deviating from that of K_b determined by UV/VIS titration (*Fig. 5*), indicating that the interaction mechanism is determined not only by complex formation but also by some weak interactions such as hydrophobic force, *Van der Waals* force, and electrostatic force [15]. More importantly, DNA intercalators have been used extensively as antitumor, antineoplastic, antimalarial, antibiotic, and antifungal agents [9]. There is a criterion for screening out antitumor drugs from others by DNA–EB fluorescent tracer method,

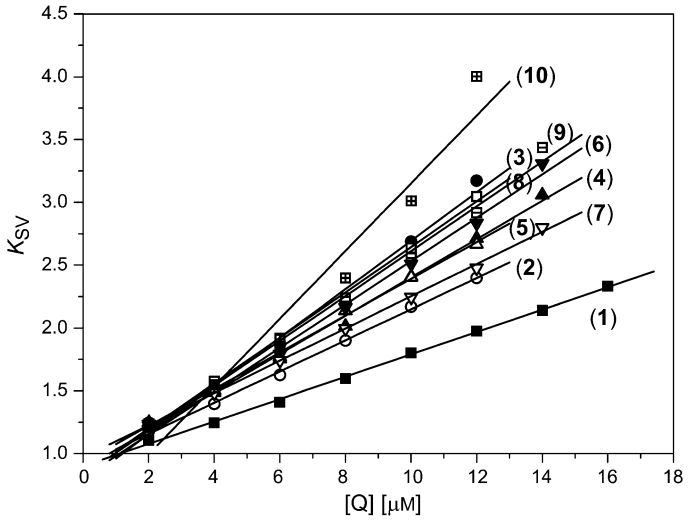

Fig. 6. *The* Stern–Volmer *plots for ligand and* Ln^{III} *complexes in EB–DNA systems.* The molar concentrations of DNA and EB are 4.0 μM (nucleotides) and 0.32 μM, respectively. $\lambda_{ex} = 525$ nm, $\lambda_{em} = 587$ nm.

i.e., a compound may be used as potential antitumor drug, if it causes a 50% loss of DNA–EB fluorescence intensity by fluorescent titrations before the molar concentration ratio of the compound to DNA (nucleotides) does not exceed 100 : 1 [16]. The FC_{50} value is introduced to denote the molar concentration of a compound that causes a 50% loss in the fluorescence intensity of DNA–EB system. According to the FC_{50} data and the molar ratios of compounds to DNA (*Table*), it is interesting to note that at FC_{50}, all the molar concentration ratios of the investigated compounds to DNA (1.431 – 3.088 : 1) are significantly under 100 : 1, indicating that all these investigated compounds can be considered as potential antitumor drugs, and the antitumor activities of Ln^{III} complexes are probably better than that of ligand. However, their pharmacodynamical, pharmacological, and toxicological properties should be further studied *in vivo*.

Fig. 7 shows the plots of HO• radical-scavenging effects [%] *vs.* molar concentration of the tested complexes. The SC_{50} value, calculated from the regression line of the log (concentration of the tested compound) *vs.* the scavenging effect [%] of the compound, is introduced to denote the molar concentration of the tested compound which causes a 50% scavenging effect on HO• radicals. The SC_{50} values of ligand and Ln^{III} complexes for HO• are 21.33 and 2.499 – 6.149 μM, respectively (*Table*). Apparently, the scavenging effects of Ln^{III} complexes on HO• are much higher than that of ligand, possibly in that the larger conjugated metal complexes can react with HO• to form larger stable macromolecular radicals by the typical H-abstraction reaction than the ligand [17]. The SC_{50} value of mannite for HO• tested under the same conditions is 14.41 mM. However, the scavenging effects of Ln^{III} complexes and ligand on HO• are much better than that of either mannite or ascorbic acid (the value of SC_{50} for HO• is 1.537 mg ml^{-1}, *i.e.*, 8.727 mM), standard antioxidative agents for nonenzymatic reaction [18]. Endowed

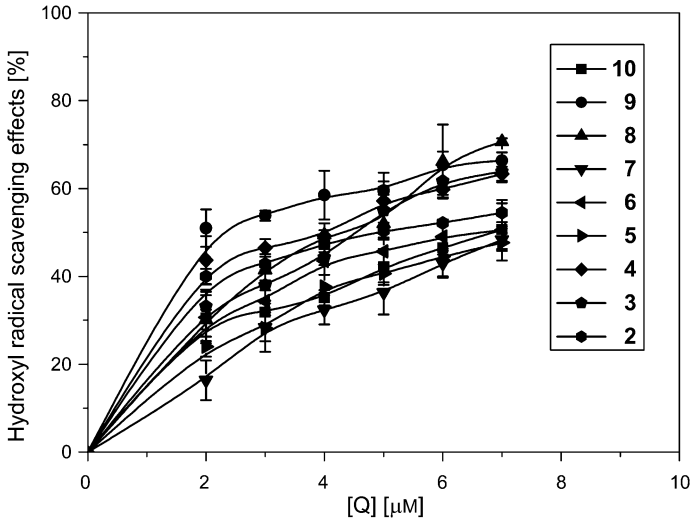

Fig. 7. *Plots of HO· radical-scavenging effects* [%] vs. *the molar concentrations of the tested complexes*

with antioxidative properties, these DNA binders may be effective inhibitors of the formation of a DNA–TBP (= TATA binding protein) complex topoisomerases.

Conclusions. – 8-Hydroxyquinoline-7-carboxaldehyde (8-HQ-7-CA) and its *Schiff* base ligand 8-hydroxyquinoline-7-carboxaldehyde benzoylhydrazone (H_2L; **1**) were prepared. Then, the nine binuclear complexes $[LnL(NO_3)(H_2O)_2]_2$, **2**–**10**, were prepared from the ligand and equivalent molar amounts of $Ln(NO_3)\cdot 6\,H_2O$ (Ln = La^{3+}, Nd^{3+}, Sm^{3+}, Eu^{3+}, Gd^{3+}, Dy^{3+}, Ho^{3+}, Er^{3+}, Yb^{3+}, resp.). Ligand acts as a dibasic tetradentate, binding to Ln^{III} through the phenolate O-atom, N-atom of quinolinato unit, and C=N group and –O–C=N– groups (enolized and deprotonated from O=C–NH–) of the benzoylhydrazine side chain. Dimerization of this monomeric unit may occur through the phenolate O-atoms leading to a central four-membered $(LnO)_2$ ring. However, the composition changes to $[LnL(NO_3)(DMF)_2]_2$ when the complex is dissolved in DMF solution.

In addition, ligand and all of the Ln^{III} complexes can bind to CT-DNA through intercalation with the binding constants at 10^5–10^6 M^{-1}, but Ln^{III} complexes present stronger affinities to DNA than the ligand. Ligand and all of the Ln^{III} complexes may be considered as potential anticancer drugs; however, their pharmacodynamical, pharmacological and toxicological properties should be further studied *in vivo*.

Moreover, ligand and all of the Ln^{III} complexes exhibit strong scavenging effects on HO· radicals, but Ln^{III} complexes show stronger scavenging effects than the ligand. Endowed with anti-oxidative properties, these DNA binders may be effective inhibitors of the formation of a DNA–TBP complex topoisomerases, which should be studied further *in vivo*. Furthermore, the Ln^{III} complexes of 8-hydroxyquinoline-7-carboxaldehyde benzoylhydrazone are similar not only in structures but also in antioxidation and DNA-binding properties with the Ln^{III} complexes of 8-hydroxyquinoline-2-carboxaldehyde benzoylhydrazone.

Experimental Part

General. Materials. Calf thymus DNA (CT-DNA) and ethidium bromide (EB) were obtained from *Sigma–Aldrich Biotech. Co.*, Ltd. The stock soln. (1.0 mM) of the investigated compound was prepared by dissolving the powdered material into appropriate amounts of DMF soln. Deionized doubly distilled H_2O and anal. grade reagents were used throughout. CT-DNA Stock soln. was prepared by dissolving the solid material in 5 mM *Tris*·HCl buffer (pH 7.20) containing 50 mM NaCl and kept over 48 h at 4°. The CT-DNA concentration in terms of base pair l^{-1} was determined spectrophotometrically by employing an extinction coefficient of $\varepsilon = 13{,}200\ M^{-1}\ cm^{-1}$ (base pair)$^{-1}$ at 260 nm, and its concentration in terms of nucleotide l^{-1} was also determined spectrophotometrically by employing an extinction coefficient of $6600\ M^{-1}\ cm^{-1}$ (nucleotide)$^{-1}$ at 260 nm [19]. The stock soln. was stored at −20°, until it was used. Working standard soln. of CT-DNA was obtained by appropriate dilution of the stock soln. in 5 mM *Tris*·HCl buffer (pH 7.20) containing 50 mM NaCl. EB was dissolved in 5 mM *Tris*·HCl buffer (pH 7.20), and its concentration was determined assuming a molar extinction coefficient of $5600\ M^{-1}\ cm^{-1}$ at 480 nm [9].

Methods. M.p.: *XT4–100X* Microscopic melting-point apparatus (Beijing, P. R. China). IR Spectra: *Nicolet Nexus 670* FT-IR spectrometer using KBr discs in the 4000–400-cm^{-1} region. ^{1}H-NMR Spectra: *Bruker Advance DRX 200*-MHz spectrometer with tetramethylsilane (TMS) as an internal standard. ESI-MS (ESI-Trap/Mass) spectra: *Bruker Esquire6000* mass spectrophotometer; HCOOH as the proton source. Elemental analyses of C, N and H: *Elemental Vario EL* analyzer. The metal ion content was determined by complexometric titration with EDTA after destruction of the complex in the conventional manner.

Viscosity titration experiments were carried out on an *Ubbelohde* viscometer in a thermostated water bath maintained at 25.00 ± 0.01°. Data were presented as $(\eta/\eta_0)^{1/3}$ *vs.* the ratio of the compound to DNA, where η is the viscosity of DNA in the presence of the compound corrected from the solvent effect, and η_0 is the viscosity of DNA alone [9].

UV/VIS Spectra were recorded using a *Perkin–Elmer Lambda* UV/VIS spectrophotometer. The UV/VIS spectra of the investigated compounds in the absence and in the presence of the CT-DNA were obtained in DMF/*Tris*·HCl buffer (5 mM, pH 7.20) containing 50 mM NaCl of 1:100 solns., resp. The binding constant (K_b) was determined according to the *Eqn. 1* [12]:

$$\frac{[DNA]}{\varepsilon_f - \varepsilon_a} = \frac{[DNA]}{\varepsilon_f - \varepsilon_b} + \frac{1}{K_b(\varepsilon_f - \varepsilon_b)} \tag{1}$$

where [DNA] is the molar concentration of DNA in base pairs, ε_a [$M^{-1}\ cm^{-1}$] is the extinction coefficient observed, ε_f [$M^{-1}\ cm^{-1}$] is the extinction coefficient of the free compound, ε_b [$M^{-1}\ cm^{-1}$] is the extinction coefficient of the compound when fully bound to DNA, and K_b is the intrinsic binding constant. The ratio of slope to intercept in the plot of [DNA]/($\varepsilon_f - \varepsilon_a$) *vs.* [DNA] gives the value of K_b.

Fluorescence spectra were recorded with a *RF–5301PC* spectrofluorophotometer (*Shimadzu*, Japan) using a 1-cm quartz cell. Both the excitation and emission band widths were 10 nm. DNA–EB Quenching assay was performed as described in [3][20]. Measurements were conducted at a constant r.t., 298 K. *Stern–Volmer* equation was used to determine the fluorescent quenching mechanism [15]:

$$F_o/F = 1 + K_q\tau_o[Q] = 1 + K_{SV}[Q] \tag{2}$$

where F_o and F are the fluorescence intensity in the absence and in the presence of a compound at [Q] concentration, resp., K_{SV} is the *Stern–Volmer* dynamic quenching constant, K_q is the quenching rate constant of bimolecular diffusion collision, and τ_o is the lifetime of free EB.

The HO$^\bullet$ radicals in aq. media were generated through the *Fenton*-type reaction [3][21]. The 5-ml mixtures contained 2.0 ml of 100 mM phosphate buffer (pH 7.4), 1.0 ml of 0.10 mM aq. safranin, 1 ml of 1.0 mM aq. EDTA–Fe^{II}, 1 ml of 3% aq. H_2O_2, and a series of quantitatively microadding solns. of the tested compound. The mixtures were incubated at 37° for 60 min in a water-bath. Absorbance at 520 nm was measured, and the solvent effect was corrected throughout. The scavenging effect of compound on HO$^\bullet$ was calculated from the following expression [22]:

$$\text{Scavenging effect [\%]} = \frac{A_{\text{sample}} - A_{\text{blank}}}{A_{\text{control}} - A_{\text{blank}}} \times 100 \quad (3)$$

where A_{sample} is the absorbance of the sample in the presence of the tested compound, A_{blank} is the absorbance of the blank in the absence of the tested compound, and A_{control} is the absorbance in the absence of the tested compound and EDTA–Fe^{II}. The data for antioxidation activities are presented as means ± SD of three determinations and followed by *Student*'s *t*-test. Differences were considered to be statistically significant if $P < 0.05$.

Preparation of 8-Hydroxyquinoline-7-carboxaldehyde. Chloropicrin (32 ml, 0.4 mol) was dropped into the EtOH soln. of 14.5 g (0.1 mol) of 8-hydroxyquinoline and 40% aq. NaOH (1 mol) soln. Refluxing the mixtures for 4 h at 65–70°, the crude product was obtained after acidification to pH 5.0–5.5 with 0.1M HCl. Salmon-pink crystals were obtained by chromatographic separation (eluent, $V_{\text{petroleum}}/V_{\text{AcOEt}}$ 40 : 1). Then, recrystallization afforded pale-orange needle-like crystals were obtained after drying in vacuum. Yield: 18% (3.1 g), M.p. 178°.

Preparation of 8-Hydroxyquinoline-7-carboxaldehyde Benzoylhydrazone (**1**). Refluxing and stirring the mixture of a 10-ml EtOH soln. of 8-hydroxyquinoline-7-carboxaldehyde (0.519 g, 3 mM) and a 10-ml 90% EtOH aq. soln. of benzoylhydrazine (0.408 g, 3 mM) for 8 h, and cooling to r.t. afforded a precipitate, which was filtered, recrystallized from 80% MeOH aq. soln., and dried in vacuum over 48 h. Pale-yellow powder. Yield: 73.4% (0.641 g). M.p. 257–259°. UV/VIS ($\lambda_{\max}$ [nm], $\varepsilon \times 10^4$ [M^{-1} cm^{-1}]): 246 (2.58), 348 (2.11). IR (KBr): 3328, 3205, 1641, 1597, 1571, 1288. ^{1}H-NMR ((D_6)DMSO, 200 MHz): 9.63–9.60 (*dd*, *J*(2,3) = 7.2, *J*(2,4) = 1.8, H–C(2)); 8.83 (*s*, C(11)H=N); 8.96–8.95 (*d*, *J* = 2.4, H–C(4)); 7.97–7.95 (*d*, *J* = 6.6, H–C(16), H–C(20)); 7.80–7.78 (*d*, *J* = 7.5, H–C(6)); 7.76–7.73 (*m*, H–C(18)); 7.62–7.53 (*m*, H–C(3), H–C(17), H–C(19)); 7.19–7.16 (*d*, *J* = 7.5, H–C(5)). ESI-TRAP-MS (DMF): 292.1 ([*M* + H]$^+$). Anal. calc. for $C_{17}H_{13}N_3O_2$: C 70.09, H 4.50, N 14.42; found: C 37.05, H 4.54, N 14.41.

Preparation of Complexes **2**–**10**. Each complex was prepared by refluxing and stirring the mixtures of a 40-ml MeOH soln. of compound **1** (0.058 g, 0.2 mM) and equimolar amounts of $Ln(NO_3)\cdot 6\,H_2O$ (Ln = La^{3+}, Nd^{3+}, Sm^{3+}, Eu^{3+}, Gd^{3+}, Dy^{3+}, Ho^{3+}, Er^{3+}, Yb^{3+}, resp.) on a water bath. After refluxing for 30 min, Et_3N (0.020 g, 0.2 mM) was added dropwise into the mixtures to deprotonate the phenolic OH substituent of 8-hydroxyquinolinato unit. Then, the mixtures were refluxed and stirred continuously for 8 h. Cooled to r.t., the precipitate was centrifuged, washed with MeOH soln., and dried in vacuum over 48 h. All the Ln^{III} complexes were yellow powders, and their melting points exceeded 300°.

Complex **2**. Yield: 86.4% (0.091 g). UV/VIS ($\lambda_{\max}$ [nm], $\varepsilon \times 10^4$ [M^{-1} cm^{-1}]): 247 (3.68), 349 (2.76). IR (KBr): 3399, 3229, 1645, 1601, 1558, 960, 633, 1094, 1386, 1465, 1317, 1031, 836, 716, 531, 428. ESI-TRAP-MS (DMF): 1278.4 ([*M* + H]$^+$), 639.7 ([*M*/2 + H]$^+$), 638.2 ([*M*/2]$^+$). Anal. calc. for $C_{34}H_{30}La_2N_8O_{14}$: C 38.80, H 2.87, N 10.65, La 26.40; found: C 38.71, H 2.85, N 10.69, La 26.48. Λ_m (cm^2 Ω^{-1} mol^{-1}; DMF): 49.0.

Complex **3**. Yield: 86.6% (0.092 g). UV/VIS: 247 (2.55), 350 (1.96). IR (KBr): 3392, 3226, 1644, 1602, 1560, 963, 633, 1095, 1386, 1466, 1320, 1034, 838, 719, 533, 436. ESI-TRAP-MS (DMF): 1283.9 ([*M* + H]$^+$), 1283.0 (*M*$^+$), 642.7 ([*M*/2 + H]$^+$). Anal. calc. for $C_{34}H_{30}N_8Nd_2O_{14}$: C 38.41, H 2.84, N 10.54, Nd 27.14; found: C 38.32, H 2.82, N 10.46, Nd 27.02. Λ_m: 42.3.

Complex **4**. Yield: 81.7% (0.088 g). UV/VIS: 262 (2.98), 348 (2.27). IR (KBr): 3402, 3227, 1645, 1603, 1561, 962, 634, 1096, 1386, 1466, 1322, 1033, 837, 720, 533, 438. ESI-TRAP-MS (DMF): 1296.9 ([*M* + H]$^+$), 1295.3 (*M*$^+$), 649.3 ([*M*/2 + H]$^+$). Anal. calc. for $C_{34}H_{30}N_8O_{14}Sm_2$: C 37.97, H 2.81, N 10.42, Sm 27.96; found: C 38.13, H 2.80, N 10.37, Sm 27.81. Λ_m: 40.5.

Complex **5**. Yield: 82.8% (0.089 g). UV/VIS: 261 (3.67), 348 (2.55). IR (KBr): 3387, 3230, 1643, 1602, 1562, 964, 642, 1098, 1388, 1468, 1321, 1001, 836, 721, 533, 436. ESI-TRAP-MS (DMF): 1301.1 ([*M* + H]$^+$), 649.0 ([*M*/2]$^+$). Anal. calc. for $C_{34}H_{30}Eu_2N_8O_{14}$: C 37.86, H 2.80, N 10.39, Eu 28.18; found: C 37.83, H 2.80, N 10.44, Eu 28.26. Λ_m: 58.2.

Complex **6**. Yield: 86.4% (0.094 g). UV/VIS: 263 (3.26), 347 (2.34). IR (KBr): 3398, 3223, 1646, 1603, 1561, 962, 634, 1097, 1385, 1467, 1323, 1031, 837, 722, 532, 441. ESI-TRAP-MS (DMF): 1310.7 ([*M* + H]$^+$), 655.4 ([*M*/2 + H]$^+$), 654.4 ([*M*/2]$^+$). Anal. calc. for $C_{34}H_{30}Gd_2N_8O_{14}$: C 37.49, H 2.78, N 10.29, Gd 28.88; found: C 37.38, H 2.77, N 10.23, Gd 28.97. Λ_m: 58.1.

Complex **7**. Yield: 83.9% (0.092 g). UV/VIS: 262 (2.16), 347 (1.60). IR (KBr): 3399, 3223, 1653, 1602, 1562, 962, 634, 1096, 1386, 1467, 1319, 1034, 836, 723, 535, 441. ESI-TRAP-MS (DMF): 1320.3 ([*M* + H]$^+$),

660.9 ([M/2+H]$^+$), 659.6 ([M/2]$^+$). Anal. calc. for $C_{34}H_{30}Dy_2N_8O_{14}$: C 37.14, H 2.75, N 10.29, Dy 29.55; found: C 37.24, H 2.75, N 10.22, Dy 29.64. Λ_m: 40.6.

Complex **8**. Yield: 83.7% (0.092 g). UV/VIS: 262 (2.37), 345 (1.72). IR (KBr): 3399, 3224, 1650, 1590, 1563, 962, 634, 1097, 1386, 1467, 1320, 1033, 836, 724, 535, 443. ESI-TRAP-MS (DMF): 1325.2 ([M+H]$^+$), 1324.3 (M^+), 663.8 ([M/2+H]$^+$), 662.9 ([M/2]$^+$). Anal. calc. for $C_{34}H_{30}Ho_2N_8O_{14}$: C 36.97, H 2.74, N 10.15, Ho 29.86; found: C 37.00, H 2.75, N 10.10, Ho 29.94. Λ_m: 45.0.

Complex **9**. Yield: 84.8% (0.094 g). UV/VIS: 262 (1.93), 345 (1.44). IR (KBr): 3409, 3226, 1649, 1592, 1562, , 964, 634, 1098, 1385, 1468, 1326, 1032, 837, 724, 534, 443. ESI-TRAP-MS (DMF): 1330.5 ([M+H]$^+$), 1329.1 (M^+), 665.5 ([M/2+H]$^+$). Anal. calc. for $C_{34}H_{30}Er_2N_8O_{14}$: C 36.82, H 2.73, N 10.10, Er 30.16; found: C 36.74, H 2.71, N 10.03, Er 30.12. Λ_m: 31.2.

Complex **10**. Yield: 83.8% (0.094 g). UV/VIS: 263 (3.23), 343 (2.37). IR (KBr): 3412, 3226, 1654, 1591, 1564, 965, 634, 1099, 1385, 1469, 1320, 1036, 836, 726, 537, 447. ESI-TRAP-MS (DMF): 1341.7 (M^+), 671.5 ([M/2+H]$^+$), 670.0 ([M/2]$^+$). Anal. calc. for $C_{34}H_{30}N_8O_{14}Yb_2$: C 36.44, H 2.70, N 10.00, Yb 30.88; found: C 36.27, H 2.70, N 10.07, Yb 30.97. Λ_m: 39.1.

This study was supported by *China NNSF* (No. 20975046) and *Gansu Educational Fund SRP* (No. 1010B-04).

REFERENCES

[1] G. Zuber, J. C. Quada Jr., S. M. Hecht, *J. Am. Chem. Soc.* **1998**, *120*, 9368; V.-S. Li, D. Choi, Z. Wang, L. S. Jimenez, M.-S. Tang, H. Kohn, *J. Am. Chem. Soc.* **1996**, *118*, 2326.

[2] S.-Y. Chiang, J. Welch, F. J. Rauscher III, T. A. Beerman, *Biochemistry* **1994**, *33*, 7033; J. M. Woynarowski, M. McHugh, R. D. Sigmund, T. A. Beerman, *Mol. Pharmacol.* **1989**, *35*, 177; A. Y. Chen, C. Yu, B. Gatto, L. F. Liu, *Proc. Natl. Acad. Sci. U.S.A.* **1993**, *90*, 8131.

[3] Y.-C. Liu, Z.-Y. Yang, *Biometals* **2009**, *22*, 733; Y.-C. Liu, Z.-Y. Yang, *J. Organomet. Chem.* **2009**, *694*, 3091; Y.-C. Liu, Z.-Y. Yang, *J. Inorg. Biochem.* **2009**, *103*, 1014; Y.-C. Liu, Z.-Y. Yang, *Inorg. Chem. Commun.* **2009**, *12*, 704; Y.-C. Liu, Z.-Y. Yang, *Eur. J. Med. Chem.* **2009**, *44*, 5080.

[4] A. A. El-Asmy, A. Z. El-Sonbati, A. A. Ba-Issa, M. Mounir, *Transition Met. Chem.* **1990**, *15*, 222; T. M. A. Ismail, *J. Coord. Chem.* **2005**, *58*, 141; Z. Zeng, L.-M. Jin, X.-Y. Jiao, C.-C. Guo, *Jingxi Huagong Zhongjianti* **2004**, *34*, 17; R.-X. Lei, Y.-C. Liu, *Baoji Wenli Xueyuan Xuebao* **2008**, *28*, 206; C. Hamada, Y. Hirano, T. Iida, *Nippon Kagaku Zassi* **1956**, *77*, 1107; R.-X Lei, J. Cheng, Y.-Y. Jia, C.-F. Liu, Y.-C. Liu, *Baoji Wenli Xueyuan Xuebao* **2010**, *30*, 24.

[5] W. J. Geary, *Coord. Chem. Rev.* **1971**, *7*, 81.

[6] J.-M. Ou-Yang, Z.-H. Tai, *Wuji Huaxue Xuebao* **1997**, *13*, 315.

[7] X.-H. Lu, Q.-Y. Lin, L.-C. Kong, X.-Q. He, *Huaxue Yanjiu Yu Yingyong* **2006**, *18*, 1380.

[8] D. S. Sigman, A. Mazumder, D. M. Perrin, *Chem. Rev.* **1993**, *93*, 2295.

[9] D. Suh, J. B. Chaires, *Bioorg. Med. Chem.* **1995**, *3*, 723; R. Palchaudhuri, P. J. Hergenrother, *Curr. Opin. Biotechnol.* **2007**, *18*, 497.

[10] S. Satyanarayana, J. C. Dabrowiak, J. B. Chaires, *Biochemistry* **1992**, *31*, 9319; B.-D. Wang, Z.-Y. Yang, P. Crewdson, D.-Q. Wang, *J. Inorg. Biochem.* **2007**, *101*, 1492.

[11] J. K. Barton, A. T. Danishefsky, J. M. Goldberg, *J. Am. Chem. Soc.* **1984**, *106*, 2172; H.-L. Lu, J.-J. Liang, Z.-Z. Zeng, P.-X. Xi, X.-H. Liu, F.-J. Chen, Z.-H. Xu, *Transition Met. Chem.* **2007**, *32*, 564.

[12] A. Wolfe, G. H. Shimer Jr., T. Meehan, *Biochemistry* **1987**, *26*, 6392; P.-X. Xi, Z.-H. Xu, X.-H. Liu, F.-J. Cheng, Z.-Z. Zeng, *Spectrochim. Acta, Part A* **2008**, *71*, 523.

[13] Y.-C. Liu, Z.-Y. Yang, J. Du, X.-J. Yao, R.-X. Lei, X.-D. Zheng, J.-N. Liu, H.-S. Hu, H. Li, *Immunobiology* **2008**, *213*, 651.

[14] L. A. Bagatolli, S. C. Kivatinitz, G. D. Fidelio, *J. Pharm. Sci.* **1996**, *85*, 1131; M.-M. Yang, P. Yang, L.-W. Zhang, *Chin. Sci. Bull.* **1994**, *9*, 31.

[15] A. Ayar, B. Mercimek, *Process Biochem.* **2006**, *41*, 1553.

[16] Z.-L. Li, J.-H. Chen, K.-C. Zhang, M.-L. Li, R.-Q. Yu, *Sci. China, Ser. B: Chem.* **1991**, *11*, 1193.

[17] J. Ueda, N. Saito, Y. Shimazu, T. Ozawa, *Arch. Biochem. Biophys.* **1996**, *333*, 377.

[18] R. Xing, H. Yu, S. Liu, W. Zhang, Q. Zhang, Z. Li, P. Li, *Bioorg. Med. Chem.* **2005**, *13*, 1387.
[19] F. Zsila, Z. Bikádi, M. Simonyi, *Org. Biomol. Chem*. **2004**, *2*, 2902.
[20] A. G. Krishna, D. V. Kumar, B. M. Khan, S. K. Rawal, K. N. Ganesh, *Biochim. Biophys. Acta – Gen. Subj.* **1998**, *1381*, 104.
[21] C. C. Winterbourn, *Biochem. J.* **1979**, *182*, 625; C. C. Winterbourn, *Biochem. J.* **1981**, *198*, 125.
[22] Z. Guo, R. Xing, S. Liu, H. Yu, P. Wang, C. Li, P. Li, *Bioorg. Med. Chem. Lett.* **2005**, *15*, 4600.

Received September 28, 2011